Study of (p,n) reaction in a wide energy range

Abstract

In this paper, the quasi-elastic scattering (p, n) reactions are studied for a wide range of target nuclei ^{13}C, ^{14}C, ^{48}Ca, ^{90}Zr and ^{208}Pb and different incident energies (35-160 MeV). The phenomenological Optical model potential and density independent approaches are used for these calculations in comparison with density dependent semi-microscopic approach. The density dependent parameters are modified to achieve the best calculations for many targets at different energy levels.

Keywords: quasi-elastic scattering, single folding, lane potential.

PACS: 24.50.+g,25.60.Bx,25.60.Lg,

1. Introduction

Examinations of the elastic and quasi-elastic scattering of neutrons and protons is one simplest way for better understanding the character of the nuclear interaction. The isospin is one important and interesting feature of the nucleon-nucleus interactions. In order to be determined, Lane [1] postulated a straightforward reliance of the nucleon-nucleus optical potential upon the isospin operators in terms of the optical model (OM). The matrix elements ensuing from this dependence are expressed in simple forms [2] for both of the (p,p), (n,n), and the (p,n) reactions.

Also, more realistic method is using the folded nucleon-nucleon (NN) interaction potential in the framework of OM. The folded potential represents the real part of the optical potential [3-5]. Within this method, antisymmetrization of the investigated system has been mulled over to incorporate the exchange terms [6].

We represent here a systematic study of the (p,n) reactions in the framework of the OM, in which the interaction potential is engendered by folding the chosen potential with the densities of the nucleus. The NN interactions are taken in the form of sums of direct and zero range exchange terms. Supplementally, phenomenological OM is used to describe the same reactions. It is an extending to our previous work [7].

2. The Lane Model

The nuclear interaction between an incident nucleon and a target with non-zero isospin has an isospin dependent part. The lane isospin dependent part is formulated as

$$\frac{4tT}{A}U_1 \ , \qquad (1)$$

where, U_1 is known as the Lane potential that contributes to both the elastic (p,p) and (n,n) scattering just as to the charge exchange (p,n) reaction. The isospin of the particle and target nucleus, are t, T, respectively and A is the mass number of the target. Thus, in a straightforward method, lane potential (isospin dependent part) is connected to optical potential to form the total nuclear nucleon-nucleus interaction as

$$U = U_o + \frac{4tT}{A} U_1 . \quad (2)$$

Knowledge of U_1 is of key enthusiasm for investigations of nuclear phenomena in which neutrons and protons are different (isovector modes). Numerous past appraisals of U_1 are liable to serious uncertainties as Distorted Wave Born Approximation (DWBA) analysis of (p,n) reactions. For instance, in the comparison of elastic nucleon scattering from different nuclei one must make assumptions [2] about the variation of nuclear geometry with A and ε $\left(\varepsilon = \frac{N-Z}{A}\right)$. It is on a fundamental level conceivable to stay away from these uncertainties by extracting U_1 from a consistent study of the elastic proton and neutron scattering and the charge exchange (p,n) reaction on the same target nucleus, at the same energy. We recall here briefly the consistent isospin coupling scheme [1] for the elastic nucleon-nucleus scattering and charge exchange (p,n) reaction exciting.

The matrix elements resulting from equation (2) give the following relationships [2].

$$U_{pp} = U_o - \frac{N-Z}{A} U_1 \quad (3)$$

$$U_{nn} = U_o + \frac{N-Z}{A} U_1 \quad (4)$$

Similarly, the transition matrix element or (p,n) form factor for the charge exchange reaction is

$$U_{pn} = \frac{2(N-Z)^{1/2}}{A} U_1 \quad (5)$$

Accordingly

$$U_{nn} - U_{pp} = \frac{2(N-Z)}{A} U_1 = (N-Z)^{1/2} U_{pn} . \quad (6)$$

The present calculations of angular distributions of the (p,n) elastic scattering cross sections were made by using the distorted-wave code DWUCK4 [8], and the optical potential is

$$U_{pp\,(nn)}(R) = N_R \left[V_{F0}(R) \pm \frac{N-Z}{A} V_{F1}(R) \right] + iW(R) , \quad (7)$$

for (n,n) , (p,p), and for (p,n) reaction

$$U_{pn}(R) = \frac{2(N-Z)^{1/2}}{A} \left[N_R V_{F1}(R) + iW(R) \right] , \quad (8)$$

where $V_{F0(1)}$ (R) is the nuclear real potential calculated by the folding procedure, including the zero range exchange part of the potential by using DFPOT code [9]. W(R) is the imaginary part of the potential including both type; volume W_V(R) and surface W_S(R).

The last outcomes for the angular distributions of scattering cross sections were gotten by changing the parameters of the imaginary part of the potential to get the best fit with the experimental values.

3. Method of Calculations

In this work, we study the quasi-elastic scattering (p,n) reaction. Differential scattering cross sections are determined for a wide range of incident proton energies by different targets. Initially, proton of energies 35, 45 and 135 MeV [10,111] incident on target nuclei ^{48}Ca. Pursued by, proton of energies 35, 45, 120 and 160 MeV [10,13,14] incidents on target nuclei ^{90}Zr. Then, proton of energies 35 and 45 MeV [9] incidents on target nucleus ^{208}Pb. At long last, proton of energies 35 and 120 MeV [15,16] incidents on target isotope nuclei ^{13}C and ^{14}C, respectively.

3.1 The phenomenological Optical potential

The global WS parameters for different nucleon potentials [17-19] have been carefully determined based on large experimental data bases of the elastic nucleon-nucleus scattering. Then, it has been found to be useful in calculation of the transition optical potential (Upn).

We have been chosen CH89 global optical parameters as initial parameters, and in that case a minor change is needed to reproduce the best fit of the scattering cross sections with the experimental data in the optical model (OM) analysis. The equations and parameters used in potential CH89 are listed in ref.[18].

3.2.1 Density independence folding potential

The nucleon-nucleus potential can be obtained by single folding (SF) the density distribution of the target nucleus $\rho_T(r)$ with the NN effective interaction V_{NN} (S) [20]

$$V_F(R) = \int \rho_T(r)\, V_{NN}(S)\, dr \ , \tag{9}$$

where, $S = |R - r|$ is the distance between the two nucleons. Here, we take the NN interaction to be density independent (DI) M3Y effective NN interaction with a zero–range approximation in the form

$$(V_0)_{NN}(S) = 7999 \ \frac{e^{-4s}}{4s} - 2134 \ \frac{e^{-2.5s}}{2.5s} - 276 \ [1 - \alpha\varepsilon\,]\,\delta(s) \ , \tag{10}$$

and

$$(V_1)_{NN}(S) = -4886 \ \frac{e^{-4s}}{4s} + 1176 \ \frac{e^{-2.5s}}{2.5s} + 228 \ [1 - \alpha\varepsilon\,]\,\delta(s) \, . \tag{11}$$

V_0 and V_1 are the (isoscalar and isovector) M3Y effective NN interaction potential respectively, supplemented by zero range potentials. Where (α) is the energy dependent parameter = 0.005 MeV^{-1}. The zero range potential (third term) in equations (10) and (11) represents the single nucleon exchange term [20].

Consequently, the real folded isoscalar $V_{F0}(R)$ and isovector $V_{F1}(R)$ components of $V_F(R)$ potentials are calculated and further scaled by a factor N_R in addition to W(R) to obtain $U_{0(1)}$. Thus,

the best fitted real folded potential in addition to WS imaginary potential parameters are listed in Tables (1-11).

3.3.1 Density dependence folding potential

The failure of simple M3Y-NN type interactions to give a good description of the data in many cases [21-24], leads to the inclusion of explicit density dependence. In consequence, the other type (DD) of the SF potential is introduced as follow

$$V_F(R) = g(\rho,\varepsilon)\int \rho_T(r)\, V_{NN}(S)\, dr \ . \qquad (12)$$

The density dependence [25] adopted is

$$g(\rho,\varepsilon) = C(1-\beta(\varepsilon)\,\rho^{n}) \ . \qquad (13)$$

The density dependent parameters C and β, can be given by the subsequent

$$\beta = \left[(1-P)\rho_{\circ}^{-n}\right]\left[(3n+1)-(n+1)P\right]^{-1} , \qquad (14)$$

$$P = (10\, m\varepsilon_{\circ})\left(\hbar^{2}k_{\circ}^{2}\right)^{-1} , \qquad (15)$$

$$k_{\circ} = \left[1.5\pi^{2}\rho_{\circ}\right]^{1/3} , \qquad (16)$$

$$C = -\left(2\hbar^{2}k_{\circ}^{2}\right)\left[5mJ_{\circ}\rho_{\circ}\left(1-(n+1)\rho_{\circ}^{n}\beta\right)\right]^{-1} , \qquad (17)$$

Where m is a nucleonic mass equal to 931.5 MeV/c^2, k_o is Fermi momentum at saturation condition. It is quite obvious that density dependence parameter (β) obtained by this method depends only on the saturation energy per nucleon ($\varepsilon_{\circ}$), the saturation density (ρ_0) and the index (n) but not on the parameters of the M3Y interaction while the parameter (C) depends on and also through the volume integral ($J_{\circ}$) of the isosaclar part of the M3Y interaction supplemented by the zero-range exchange potential having the form

$$J_{\circ} = \int (V_{\circ})_{NN}(S)\, d^{3}S \ . \qquad (18)$$

As a result, the two parameters β and C are chosen to have different values with different investigated energies. Thus, the density dependent factor g(ρ,ε) is turned out to be function of energy. The value of parameter n= 2/3 was firstly taken by Myers in the SF calculation [25].Three forms are applied in our analysis which is summarized according to energy range used as:

$$g(\rho,\varepsilon) = 2.07(1-1.667\,\rho^{2/3}) \qquad (19)$$

this denoted as DD1 within energy range 120-160 MeV, where $\rho_0 = 0.15$ [26,27],

$$g(\rho,\varepsilon) = 2.85(1-1.614\,\rho^{2/3}) \qquad (20)$$

this indicated as DD2 at energy 45 MeV, where $\rho_0 = 0.16$ [28,29], and

$$g(\rho,\varepsilon) = 1.55(1 - 1.054\,\rho^{2/3}), \quad (21)$$

this is referred to as DD3 at energy 35 MeV, where $\rho_0 = 0.28$ [30,31].

Notice that, g(ρ,ε) in equation (13) is a function of energy at only one value at saturation. Then it was our trial to be obtained as a variable function with changing energy. According to the investigated results, it is appropriate to improve the value of ρ_0 to be as a function in energy to generalize and achieve the three ranges. This is represented by:

$$\rho_{\circ} = 10^{-8} E^{4} - 5\times 10^{-6} E^{3} + 8\times 10^{-4} E^{2} - 0.058\,E + 1.47\ . \quad (22)$$

Consistent with the above formula, it is proper to draw the relation that shows the variation of ρ_0 with E in the figure (1) as following:

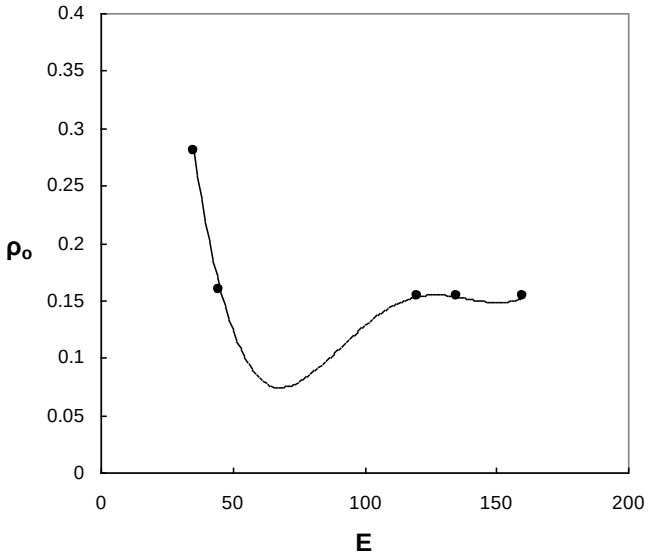

Fig.(1): The variation of different values of saturation density (ρ_0) with different energies (E).

Summarizing that, we are used the SF program to calculate the real parts of the nucleon-nucleus scattering of several systems. The interactions are divided into density independence M3Y-DI and density dependence DD1, DD2 and DD3 interaction. From the above description, the basic inputs to a folding calculation are nuclear densities of the target nuclei and the effective NN interaction. The densities of ^{13}C and ^{14}C are taken as Gaussian [32], ^{48}Ca [33], ^{90}Zr [34] and ^{208}Pb [35] are taken as Fermi. In the present work, we examine a few representative cases about the real part of nuclear potential. These data are very helpful to test the modified density dependent Folding potential.

4. Results and Conclusion

In this work, the phenomenological OM and semi-microscopic (SF) model are used. The DI and DD1, DD2 and DD3 effective NN interaction is employed to drive the real folding optical model potentials of the investigated systems, assuming the density distribution for different targets nuclei. The imaginary potentials are supplemented to the derived potentials in phenomenological Woods-Saxon (WS) form. The quasi-elastic angular distributions for the different systems are calculated and the results are compared to the experimental data.

The Figures (2-12) show the cross section data for the quasi elastic scattering using different potentials for the investigated nuclei at low and high energies. It is easy to notice from these figures that, all the used potentials give a good results in a comparison with others work as in ref. [36-38] for the scattering cross sections of each of the reactions (p,n), although these potentials have different characteristic values. This is due to the fact that the calculations of the interaction cross sections depend also up on the imaginary potential.

In harmony with the success of density and energy dependent in the analysis of quasi-elastic scattering (p,n) reaction, it is interested to study how far the calculated Unn and Upp are consistent with Upn in equation (5). So, the calculations were done to get Unn and Upp by changing the potential according to equations (3) and (4). The Unn, Upp and Upn characteristics of the investigated nuclei for the used potentials are presented in Tables (1-11).

Generally, we concluded that using the modified density dependent single folding model successfully describes the quasi-elastic scattering experimental data at different energy ranges and gives a good agreement of the calculated values of Unn and Upp with equation (5).

References

[1] A.M. Lane. Nucl.Phys. 35, 676 (1962).

[2] J.R. Carlson, C.D. Zafiratos Nucl. Phys. A., 249, 29 (1975).

[3] G.R. Satchler, K.W. Mcvoy, Nucl. Phys. A, 522: 621 (1991).

[4] E.E. Arellano, Phys. Rev. C 66:24602(2002).

[5] A.A.Ogloblin, Yu.Aglukhov, Phys. Rev. C 62: 44601 (2000).

[6] D.T.Khoa, G.R.Satchler Nucl. Phys.A 668:3 (2000).

[7] A. El-Nohy, H. A. Motaweh, A. Attia , M. N. El-Hammamy, 20th International Seminar on Interaction of Neutrons with Nuclei: Alushta, Ukraine, 21–26 May (2012).

[8] J.Kunz, Abstract number NESC9872, 36 (1987).

[9] J.Cook, Comput. Phys. Comm. 25,125 (1982).

[10] R.R. Doering, D.M. Patterson,A. Galonsky, Phys. Rev. C 12, 378 (1975).
[11] E. Bainum, J. Rapaport, C. D. Goodman et al., Phys. Rev. Lett. 44, 1751 (1980).
[12] E. Sugarbaker et al., Proceedings of the International Conference on Nuclear Structure, Amsterdam, 1982, edited by A. Van Der Wonde and B. J. Verhaar, pp. 77.
Jacob Rapaport (private communication)
[13] T. Orihara, T. Murakami, Nucl. Instrum. Methods 181, 15 (1981).
[14] T. Oriharaet al., Nucl. Instrum. Methods Phys. Res. A257, 189 (1987).
[15] Jacob Rapaport, unpublished (private communication).
[16] D.Anderson, M.Mostajabodda'vati, C.Lebo et al., Phys.Rev.C43,1630 (1991).
[17] D.Becheetti, G.W.Greenlees, Phys.Rev. 182,1190(1969).
[18] L.Varner,W.J.Thompson, T.L.McAbee, E.J.Ludwig,T.B.Clegg, Phys.Rep. 201,57 (1991).
[19] A.J.Koning, J.P.Delaroche, Nucl.Phys. A713,231(2003)
[20] R. Satchler,W G Love, Phys. Rep. 55,183 (1979).
[21] G.Bohlen , M.R.Clover, G. Ingold et al. ,Z. Phys.A 308,121(1982).
[22] G.Bohlen , X.S.CHEN, J.G.Cramer et al, Z. Phys. A 322, 241(1985).
[23] Stiliaris, H.G.Bohlen, P.Frobrich et al., Phys. Lett. B223, 291(1989).
[24] N.Basu, P. Roy Chowdhury, C. Samanta, Acta Physica Polonia B 37 (10), 2869 (2006).
[25] W.D. Myers, Nucl. Phys. A204, 465 (1973).
[26] Bandyopadhyay, C. Samanta, S.K. Samaddar, J.N. De, Nucl. Phys. A511,1 (1990).
[27] Roy Chowdhury, C. Samanta, D.N. Basu, Mod. Phys. Letts. A21, 1605(2005).
[28] Audi, A.H. Wapstra, C. Thibault, Nucl. Phys. A729, 337 (2003).
[29] Satpathy, V.S. Uma Maheswari, R.C. Nayak, Phys. Rep. 319, 85 (1999).
[30] Schutz et. al., Nucl. Phys. A599, 97c (1996).
[31] Friedman, V.R. Pandharipande, Nucl. Phys. A361, 502 (1981).
[32] Ozawa et al., Nucl.Phys.A 691, 599(2001).
[33] De Veries, and C.W.De Jager, Nucl. Data Tables 36, (1987) 495.
[34] El-AzabFarid , M.A.Hassanain, Nucl.Phys. A678, 39 (2000).
[35] Umemoto, S.Hirenzaki, K.Kume, H.Toki, Phys. Rev. C62, 024606 (2000).
[36] Osman, Acta Physica Polonica B 40,2345(2009).
[37] F. Arellano, W.G.Love, arXiv: 0706.2523 v1 [nucl-th] (2007).
[38] T.Khoa, H. S. Than, D. C. Cuong, arXiv: 0706.1282 v1 [nucl-th] (2007).

Table 1: The best-fit parameters of the folded real potential in addition to Woods-Saxon imaginary potentials to (p,n) data of ^{90}Zr at 35 MeV within different models

Model	Channel	N_R	V MeV	r fm	a fm	W_v MeV	R_v fm	a_v fm	W_s MeV	R_s Fm	a_s fm
OM	(p,p)	---	70.97	1.062	0.8563	0.966	1.47	0.69	6.785	1.27	0.69
	(n ,n)		14.21	1.052	0.8454	0.696	1.27	0.69	5.878	1.27	0.69
	(p,n)		1.73	1.045	0.8795	1.326	1.16	0.69	0.00	0.00	0.00
DI	(p,p)	2.64	66.97	1.0427	0.8263	0.166	1.37	0.69	6.785	1.27	0.69
	(n ,n)	0.53	12.21	1.0427	0.8254	0.096	1.27	0.69	5.878	1.27	0.69
	(p,n)	2.30	1.830	1.0356	0.8595	1.366	1.17	0.69	0.00	0.00	0.00
DD1	(p,p)	1.86	71.97	1.0429	0.8263	0.866	1.47	0.69	6.785	1.27	0.69
	(n ,n)	0.41	14.21	1.0427	0.8254	0.596	1.27	0.69	5.878	1.27	0.69
	(p,n)	1.59	1.930	1.0360	0.8622	1.356	1.17	0.99	0.00	0.00	0.00
DD3	(p,p)	2.10	75.00	1.0427	0.8294	0.966	1.37	0.69	6.785	1.27	0.69
	(n ,n)	0.53	15.81	1.0431	0.8256	0.956	1.37	0.69	5.878	1.27	0.69
	(p,n)	1.89	1.930	1.0358	0.8611	1.206	1.17	0.69	0.00	0.00	0.00

Table 2: The best-fit parameters of the folded real potential in addition to Woods-Saxon imaginary potentials to (p,n) data of ^{90}Zr at 45 MeV within different models

Model	Channel	N_R	V MeV	r fm	a fm	W_v MeV	R_v fm	a_v fm	W_s MeV	R_s Fm	a_s fm
OM	(p,p)	---	68.72	1.049	0.8431	3.052	1.27	0.69	5.974	1.27	0.69
	(n ,n)		23.62	1.050	0.8380	3.080	1.27	0.69	5.098	1.27	0.69
	(p,n)		1.277	1.038	0.8875	1.152	1.29	0.69	0.00	0.00	0.00
DI	(p,p)	0.83	69.72	1.0391	0.8431	3.052	1.27	0.69	5.974	1.27	0.69
	(n ,n)	0.29	22.62	1.0402	0.8380	3.080	1.27	0.69	5.098	1.27	0.69
	(p,n)	0.46	1.177	1.0289	0.8875	1.152	1.29	0.69	0.00	0.00	0.00
DD1	(p,p)	1.11	75.72	1.0425	0.8467	6.052	1.27	0.69	5.974	1.27	0.69
	(n ,n)	0.42	25.62	1.0431	0.8421	4.080	1.27	0.69	5.098	1.27	0.69
	(p,n)	0.75	1.557	1.0324	0.8932	1.552	1.27	0.69	0.00	0.00	0.00
DD2	(p,p)	0.75	73.72	1.042	0.8466	6.052	1.27	0.99	5.97	1.27	0.69
	(n ,n)	0.28	24.62	1.0431	0.8412	4.080	1.27	0.99	5.09	1.27	0.69
	(p,n)	0.56	1.677	1.0322	0.8928	1.502	1.28	0.69	0.00	0.00	0.00

Table 3: The best-fit parameters of the folded real potential in addition to Woods-Saxon imaginary potentials to (p,n) data of ^{90}Zr at 120 MeV within different models

Model	Channel	N_R	V MeV	r fm	a fm	W_v MeV	R_v fm	a_v fm	W_s MeV	R_s Fm	a_s fm
OM	(p,p)	---	52.56	0.9663	1.057	7.73	1.27	0.69	1.338	1.27	0.69
	(n ,n)		31.84	1.203	0.9018	7.76	1.27	0.69	1.123	1.27	0.69
	(p,n)		1.905	0.885	1.277	0.38	1.27	0.69	0.00	0.00	0.00
DI	(p,p)	0.83	50.16	0.9963	1.007	7.730	1.27	0.69	1.388	1.27	0.69
	(n ,n)	0.55	30.59	1.0039	0.9818	7.760	1.27	0.69	1.123	1.27	0.69
	(p,n)	1.38	1.885	0.8557	1.377	0.430	1.27	0.69	0.00	0.00	0.00
DD1	(p,p)	1.25	50.16	0.9514	1.166	7.730	1.27	0.69	1.388	1.27	0.69
	(n ,n)	0.84	30.59	0.9584	1.146	7.760	1.57	0.69	1.123	1.27	0.69
	(p,n)	1.79	1.985	0.8588	1.394	0.350	1.27	0.69	0.00	0.00	0.00

Table 4: The best-fit parameters of the folded real potential in addition to Woods-Saxon imaginary potentials to (p,n) data of ^{90}Zr at 160 MeV within different models

Model	Channel	N_R	V MeV	r fm	a fm	W_v MeV	R_v fm	a_v fm	W_s MeV	R_s Fm	a_s fm
OM	(p,p)	---	60.50	0.951	1.273	5.794	1.27	0.99	0.509	1.27	0.69
	(n ,n)		38.81	0.951	1.158	8.196	2.27	0.59	0.406	1.27	0.69
	(p,n)		0.456	0.965	2.646	1.124	1.17	0.99	0.00	0.00	0.00
DI	(p,p)	0.96	61.90	0.9414	1.173	5.794	1.27	0.99	0.509	1.27	0.69
	(n ,n)	0.58	35.41	0.961	1.118	8.196	2.27	0.59	0.406	1.27	0.69
	(p,n)	0.06	0.356	0.955	2.546	1.124	1.17	0.89	0.00	0.00	0.00
DD1	(p,p)	1.59	55.90	0.9476	1.198	8.794	0.17	0.99	0.509	1.27	0.69
	(n ,n)	1.06	35.41	0.9673	1.140	8.196	0.37	0.69	0.406	1.27	0.69
	(p,n)	0.008	0.146	2.249	2.805	0.694	1.10	0.99	0.00	0.00	0.00

Table 5: The best-fit parameters of the folded real potential in addition to Woods-Saxon imaginary potentials to (p,n) data of ^{13}C at 35 MeV within different models

Model	Channel	N_R	V MeV	r fm	a fm	W_v MeV	R_v fm	a_v fm	W_s MeV	R_s Fm	a_s fm
OM	(p,p)	---	65.58	0.694	0.631	1.238	1.25	0.49	4.490	1.15	0.69
	(n ,n)		55.82	0.692	0.630	1.600	1.25	0.69	5.769	1.65	0.69
	(p,n)		0.784	0.635	0.658	2.700	1.43	1.10	0.00	0.00	0.00
DI	(p,p)	0.64	50.58	0.7944	0.7314	1.238	1.25	0.49	4.490	1.15	0.69
	(n ,n)	0.62	45.82	0.7927	0.7300	1.600	1.25	0.69	5.769	1.65	0.69
	(p,n)	0.12	0.584	0.8254	0.7389	2.700	1.44	0.95	0.00	0.00	0.00
DD1	(p,p)	0.66	48.98	0.8084	0.7315	1.638	0.55	0.69	4.49	1.15	0.69
	(n ,n)	0.65	45.02	0.8059	0.7309	1.600	2.55	0.69	5.76	1.15	0.69
	(p,n)	0.17	0.784	0.8505	0.7359	5.638	1.05	0.89	0.00	0.00	0.00
DD3	(p,p)	0.83	42.98	0.9530	0.7434	1.638	1.55	0.69	4.49	1.15	0.69
	(n ,n)	0.82	40.02	0.9488	0.7439	1.600	1.55	0.69	5.76	1.15	0.69
	(p,n)	0.09	0.284	1.0058	0.7393	6.638	0.98	0.89	0.00	0.00	0.00

Table 6: The best-fit parameters of the folded real potential in addition to Woods-Saxon imaginary potentials to (p,n) data of ^{14}C at 120 MeV within different models

Model	Channel	N_R	V MeV	r fm	a fm	W_v MeV	R_v fm	a_v fm	W_s MeV	R_s Fm	a_s fm
OM	(p,p)	---	39.50	1.255	0.650	8.756	1.25	0.69	1.239	1.15	0.69
	(n ,n)		22.50	1.177	0.669	5.761	1.25	0.69	0.936	1.15	0.69
	(p,n)		0.097	1.840	0.256	3.856	0.87	0.79	0.00	0.00	0.00
DI	(p,p)	1.22	35.50	1.1559	0.6001	8.756	1.25	0.69	1.239	1.15	0.69
	(n ,n)	0.67	20.50	1.0776	0.6494	5.761	1.25	0.69	0.936	1.15	0.69
	(p,n)	0.17	0.067	1.8409	0.2167	3.856	0.87	0.79	0.00	0.00	0.00
DD1	(p,p)	1.01	29.50	1.1551	0.6013	8.756	1.25	0.69	1.239	1.15	0.69
	(n ,n)	1.00	30.50	1.0775	0.6481	5.761	1.25	0.69	0.936	1.55	0.69
	(p,n)	0.25	0.097	1.8413	0.2216	3.856	0.87	0.79	0.00	0.00	0.00

Table 7: The best-fit parameters of the folded real potential in addition to Woods-Saxon imaginary potentials to (p,n) data of ^{48}Ca at 35 MeV within different models

Model	Channel	N_R	V MeV	r fm	a fm	W_v MeV	R_v fm	a_v fm	W_s MeV	R_s Fm	a_s fm
OM	(p,p)	---	36.16	1.158	0.69	3.27	1.11	0.69	7.073	1.11	0.69
	(n ,n)		32.79	1.158	0.69	3.90	1.11	0.69	3.420	1.11	0.69
	(p,n)		1.100	1.158	0.69	3.42	1.21	0.69	0.00	0.00	0.00
DI	(p,p)	1.08	70.27	0.9870	0.8826	2.270	1.21	0.69	7.073	1.11	0.69
	(n ,n)	0.64	35.85	0.9881	0.8782	2.900	1.21	0.69	3.420	1.11	0.69
	(p,n)	0.67	2.230	0.9779	0.9128	2.270	1.21	0.60	0.00	0.00	0.00
DD1	(p,p)	0.88	60.12	0.9966	0.8986	6.110	1.11	0.69	8.073	1.11	0.69
	(n ,n)	0.88	51.29	0.9977	0.8934	8.900	1.11	0.69	7.420	1.11	0.69
	(p,n)	0.25	0.882	0.9875	0.9304	4.100	1.21	0.55	0.00	0.00	0.00
DD3	(p,p)	0.89	62.12	0.9911	0.8905	4.510	1.11	0.69	0.173	1.11	0.69
	(n ,n)	0.76	45.29	0.9927	0.8849	8.110	1.11	0.69	5.42	1.11	0.69
	(p,n)	0.28	0.982	0.9820	0.9215	2.900	1.25	0.59	0.00	0.00	0.00

Table 8: The best-fit parameters of the folded real potential in addition to Woods-Saxon imaginary potentials to (p,n) data of ^{48}Ca at 45 MeV within different models

Model	Channel	N_R	V MeV	r fm	a fm	W_v MeV	R_v fm	a_v fm	W_s MeV	R_s Fm	a_s fm
OM	(p,p)		56.46	0.964	0.7512	1.184	1.21	0.69	6.163	1.11	0.69
	(n ,n)	---	41.81	0.924	0.9207	1.18	1.21	0.69	5.383	1.11	0.69
	(p,n)		0.145	1.054	0.1445	2.88	1.25	0.69	0.00	0.00	0.00
DI	(p,p)	0.89	60.46	0.9647	0.7812	1.184	1.21	0.69	6.163	1.11	0.69
	(n ,n)	0.62	40.81	0.9248	0.9107	1.180	1.21	0.69	5.383	1.11	0.69
	(p,n)	0.16	0.245	1.0549	0.1345	2.880	1.10	0.69	0.00	0.00	0.00
DD1	(p,p)	0.97	62.16	0.9724	0.7934	1.770	1.21	0.69	6.163	1.11	0.69
	(n ,n)	0.64	39.79	0.9319	0.9309	1.280	1.21	0.69	5.420	1.11	0.69
	(p,n)	0.14	0.200	1.0566	0.1329	2.520	1.21	0.69	0.00	0.00	0.00
DD2	(p,p)	0.57	48.16	1.040	06966	0.770	0.85	0.39	6.163	1.11	0.69
	(n ,n)	0.52	42.09	1.026	0.8091	2.780	1.21	0.69	5.42	1.11	0.69
	(p,n)	0.09	0.20	1.0563	0.1331	4.520	1.00	0.89	0.00	0.00	0.00

Table 9: The best-fit parameters of the folded real potential in addition to Woods-Saxon imaginary potentials to (p,n) data of ^{48}Ca at 135 MeV within different models

Model	Channel	N_R	V MeV	r fm	a fm	W_v MeV	R_v fm	a_v fm	W_s MeV	R_s Fm	a_s fm
OM	(p,p)	---	40.16	1.158	0.69	2.27	1.11	0.69	7.073	1.11	0.69
	(n ,n)		20.79	1.158	0.69	2.90	1.11	0.69	3.420	1.11	0.69
	(p,n)		0.100	1.158	0.69	1.22	1.11	0.79	0.00	0.00	0.00
DI	(p,p)	1.27	60.80	0.8755	1.041	2.77	1.11	1.19	0.950	1.11	0.69
	(n ,n)	0.68	30.10	0.8917	0.997	7.780	1.21	0.89	0.449	1.11	0.69
	(p,n)	0.06	0.10	0.4344	1.785	1.670	1.01	0.79	0.00	0.00	0.00
DD1	(p,p)	0.93	42.16	0.8818	1.071	1.270	1.11	0.69	7.073	1.11	0.69
	(n ,n)	0.58	24.09	0.8992	1.020	1.90	1.11	0.69	3.420	1.11	0.69
	(p,n)	0.73	1.300	0.3351	1.968	1.120	1.11	0.69	0.00	0.00	0.00

Table 10: The best-fit parameters of the folded real potential in addition to Woods-Saxon imaginary potentials to (p,n) data of ^{208}Pb at 35 MeV within different models

Model	Channel	N_R	V MeV	r fm	a fm	W_v MeV	R_v fm	a_v fm	W_s MeV	R_s Fm	a_s fm
OM	(p,p)	---	41.50	1.079	0.848	5.274	1.23	0.69	5.302	1.25	0.69
	(n ,n)		9.50	1.080	0.852	5.670	1.24	0.69	6.909	1.25	0.69
	(p,n)		1.552	1.076	0.854	2.474	1.04	0.57	0.00	0.00	0.00
DI	(p,p)	0.61	40.50	1.0896	0.8382	5.074	1.25	0.69	5.302	1.25	0.69
	(n ,n)	0.16	8.500	1.0902	0.8320	5.570	1.25	0.69	6.909	1.25	0.69
	(p,n)	0.75	1.352	1.0864	0.8644	2.574	1.01	0.55	0.00	0.00	0.00
DD1	(p,p)	0.55	38.50	1.0896	0.8398	3.074	1.75	0.89	5.302	1.25	0.69
	(n ,n)	0.25	14.50	1.0904	0.8333	3.570	1.55	0.89	6.909	1.25	0.69
	(p,n)	0.85	1.600	1.0864	0.8683	3.974	1.00	0.58	0.00	0.00	0.00
DD3	(p,p)	2.11	37.65	1.0887	0.8468	3.374	1.35	0.89	8.302	1.25	0.69
	(n ,n)	2.44	12.53	1.0936	0.7985	3.800	1.35	0.89	6.909	1.25	0.69
	(p,n)	0.13	0.250	1.0864	0. 867	3.074	1.01	0.55	0.00	0.00	0.00

Table 11: The best-fit parameters of the folded real potential in addition to Woods-Saxon imaginary potentials to (p,n) data of ^{208}Pb at 45 MeV within different models

Model	Channel	N_R	V MeV	r fm	a fm	W_v MeV	R_v fm	a_v fm	W_s MeV	R_s Fm	a_s fm
OM	(p,p)	---	68.60	1.058	0.870	5.59	1.05	0.89	7.38	1.25	0.69
	(n ,n)		66.50	1.048	0.862	5.68	1.05	0.89	5.99	1.25	0.69
	(p,n)		2.35	1.053	0.858	2.29	1.19	0.79	0.00	0.00	0.00
DI	(p,p)	1.07	68.10	1.0881	0.8506	5.591	1.05	0.89	7.38	1.25	0.69
	(n ,n)	1.29	67.50	1.0889	0.8429	5.680	1.05	0.89	5.99	1.25	0.69
	(p,n)	1.53	2.55	1.0832	0.8881	2.291	1.20	0.79	0.00	0.00	0.00
DD1	(p,p)	1.07	70.61	1.0881	0.8523	5.791	1.01	0.85	7.38	1.25	0.69
	(n ,n)	1.15	65.03	1.0891	0.8455	5.980	1.01	0.85	6.03	1.25	0.69
	(p,n)	0.83	2.723	1.0833	0.8902	2.191	1.20	0.85	0.00	0.00	0.00
DD2	(p,p)	0.85	79.61	1.0882	0.852	3.791	1.20	0.65	7.388	1.25	0.69
	(n ,n)	0.45	36.03	1.0891	0.8458	0.980	1.20	0.65	6.030	1.25	0.69
	(p,n)	0.33	1.523	1.0833	0.890	0.911	1.31	0.75	0.00	0.00	0.00

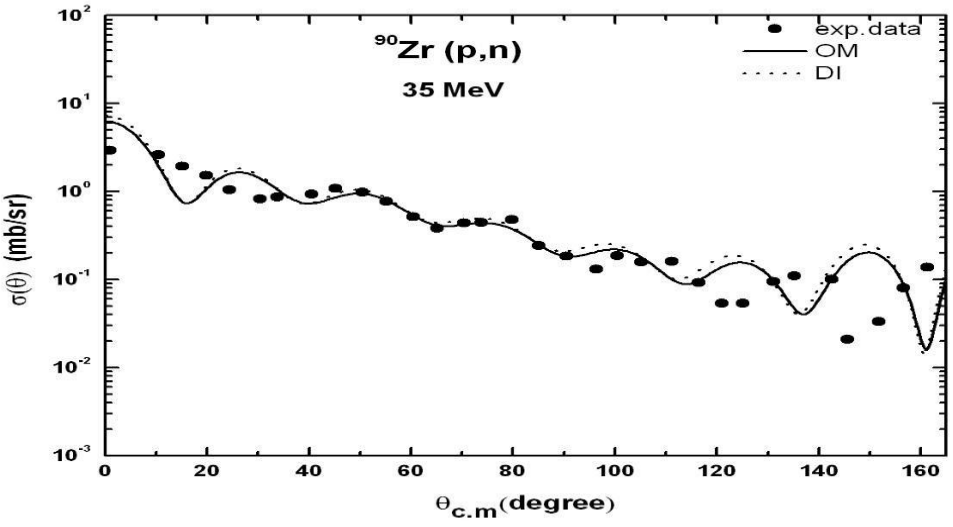

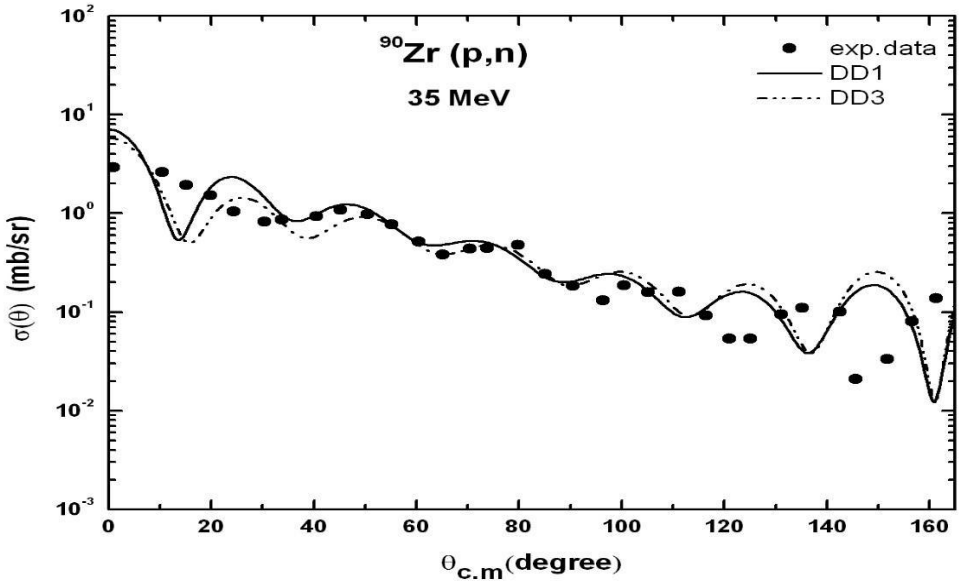

Fig. (2): Quasi-elastic scattering for ^{90}Zr (p,n) at 35 MeV.

The data are taken from Ref.[10].

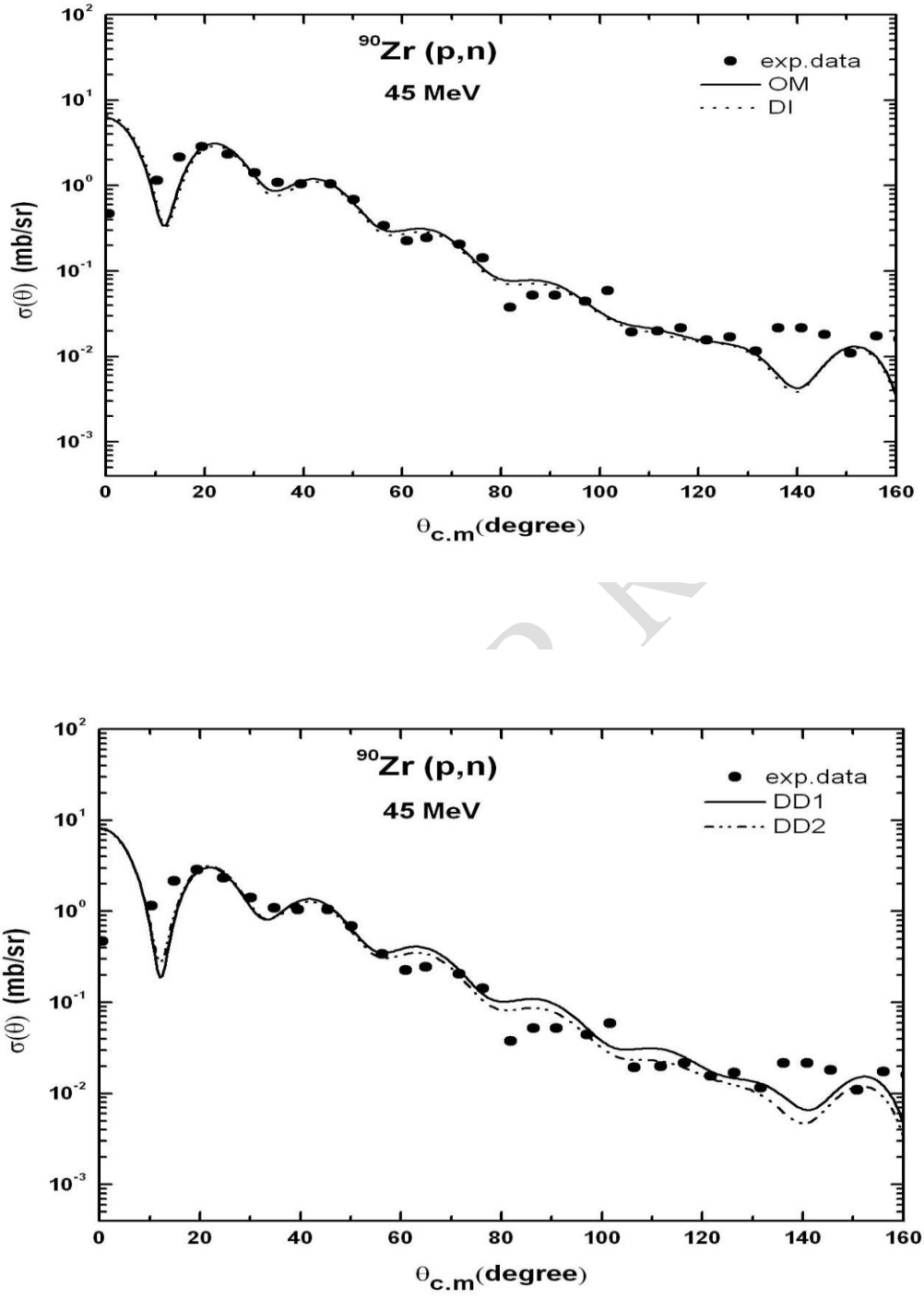

410

411 Fig. (3): Quasi-elastic scattering for ^{90}Zr (p,n) at 45 MeV.

412 The data are taken from Ref.[10].

413

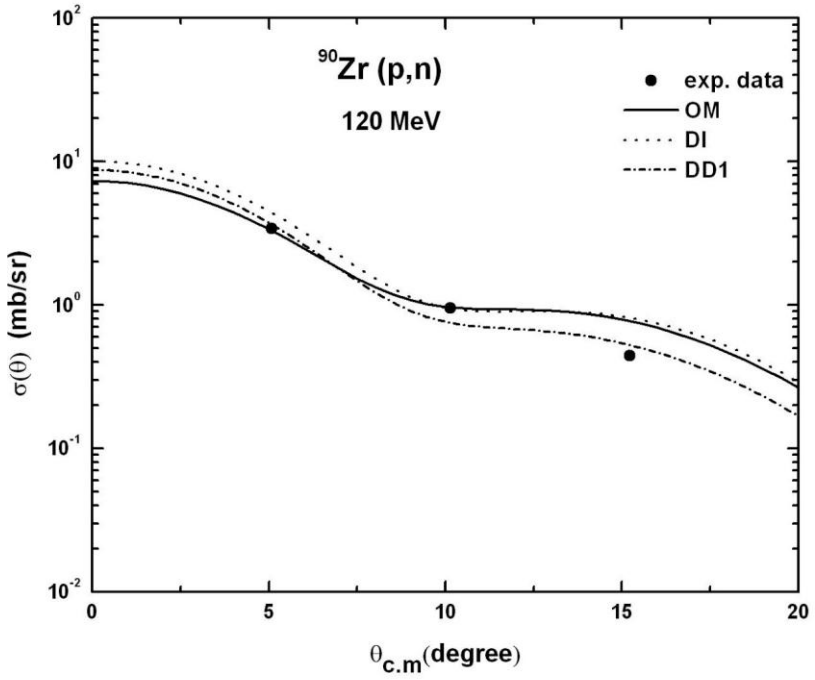

414
415 Fig. (4): Quasi-elastic scattering for ^{90}Zr (p,n) at 120 MeV.

416 The data are taken from Ref.[11].

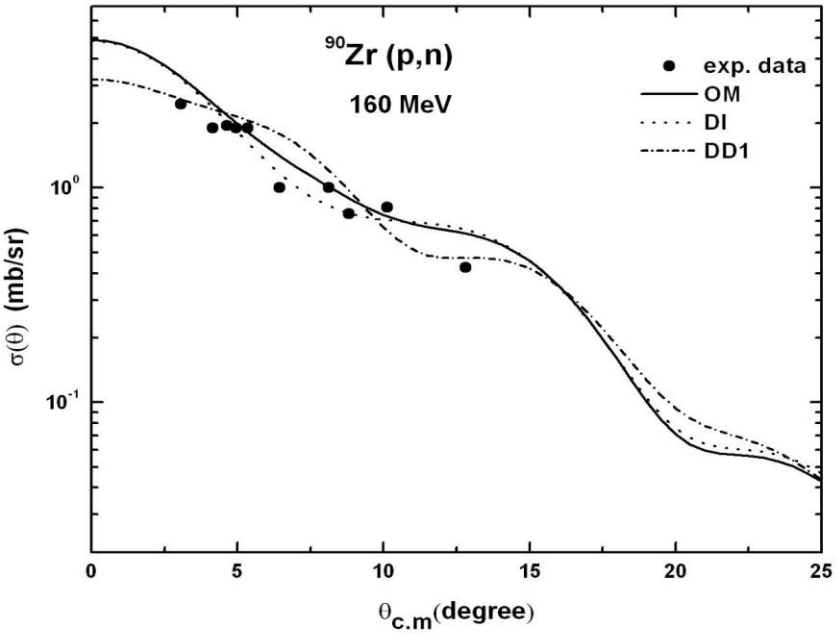

417

418 Fig. (5): Quasi-elastic scattering for ^{90}Zr (p,n) at 160 MeV.

The data are taken from Ref.[12].

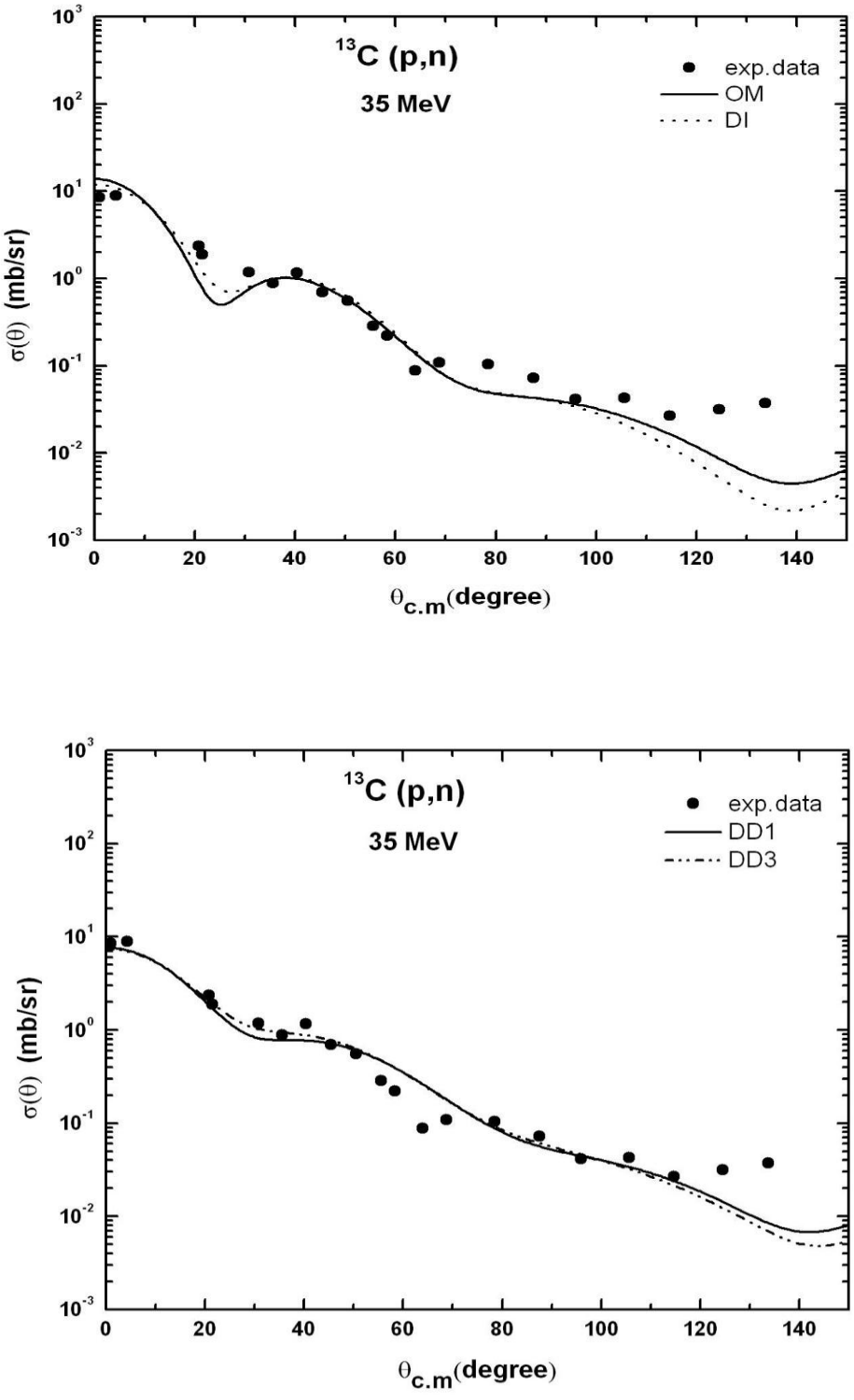

Fig (6): Quasi-elastic scattering for ^{13}C(p,n) at 35 MeV.

The data are taken from Ref. [13,14].

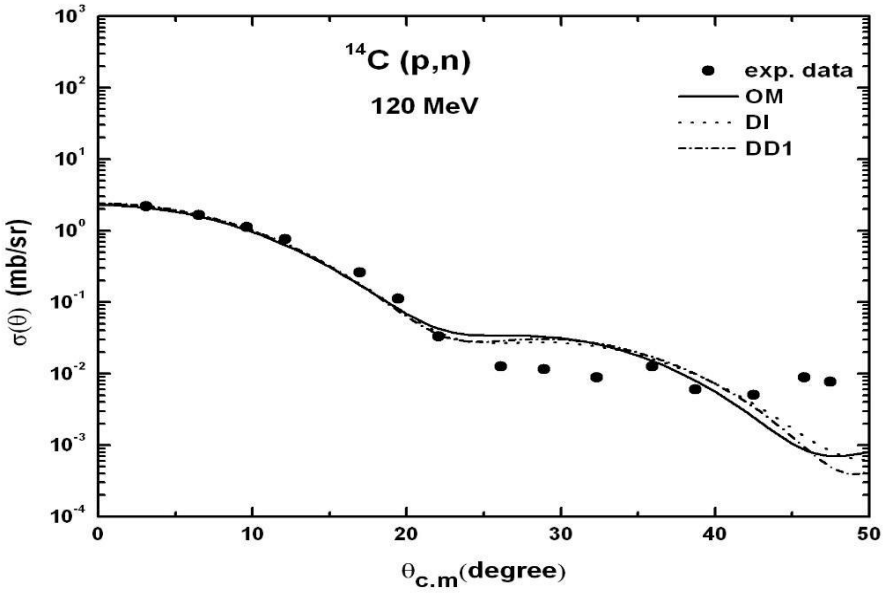

Fig (7): Quasi-elastic scattering for ^{14}C(p,n) at 120 MeV.

The data are taken from Ref.[15].

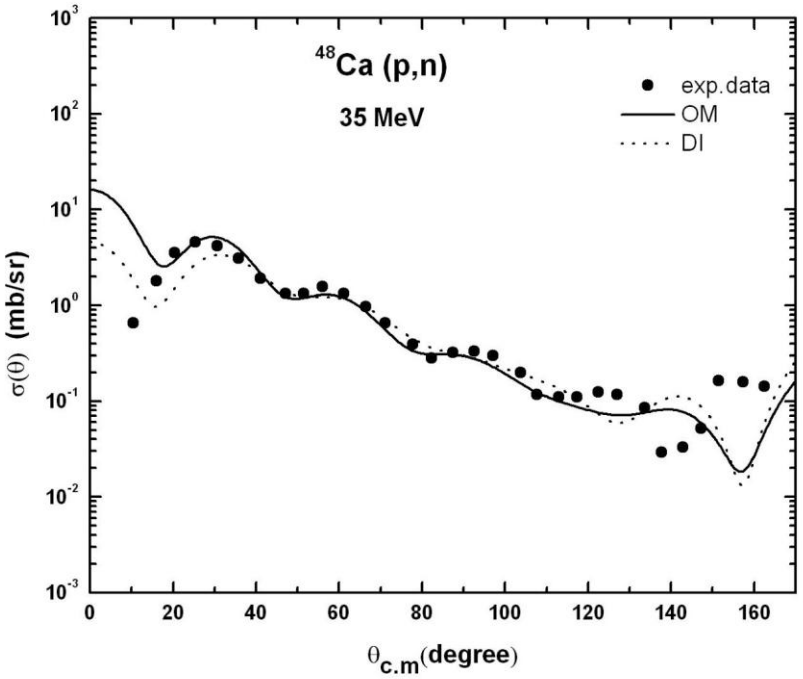

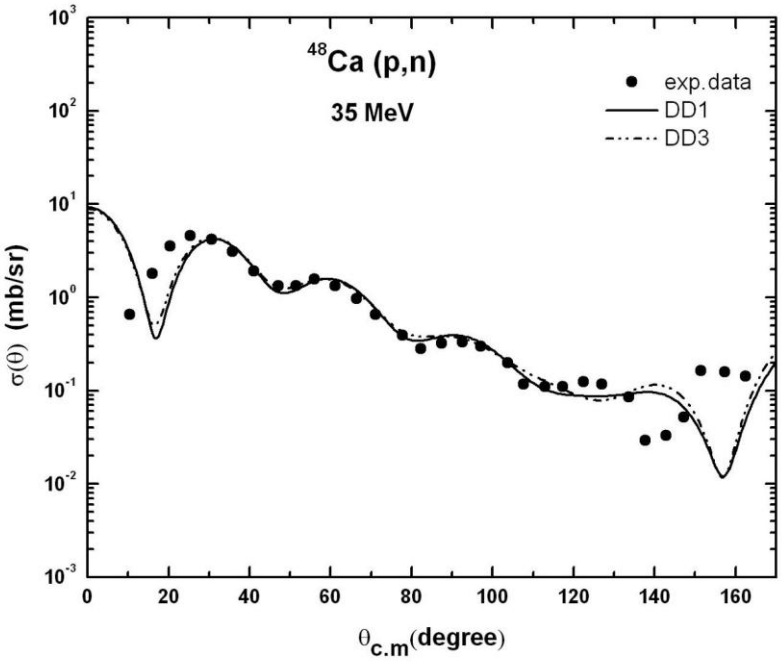

Fig. (8): Quasi-elastic scattering for ^{48}Ca (p,n) at 35 MeV.

The data are taken from Ref.[10].

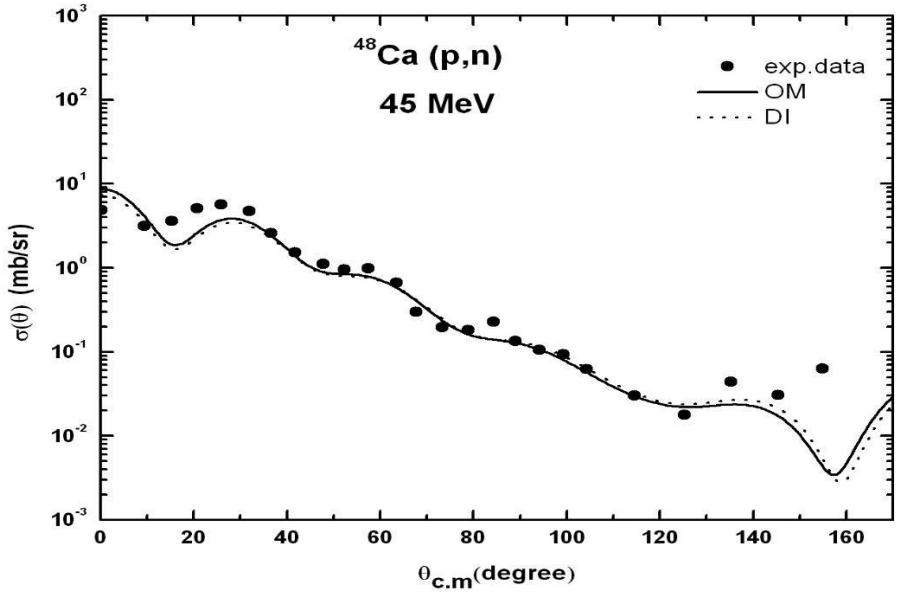

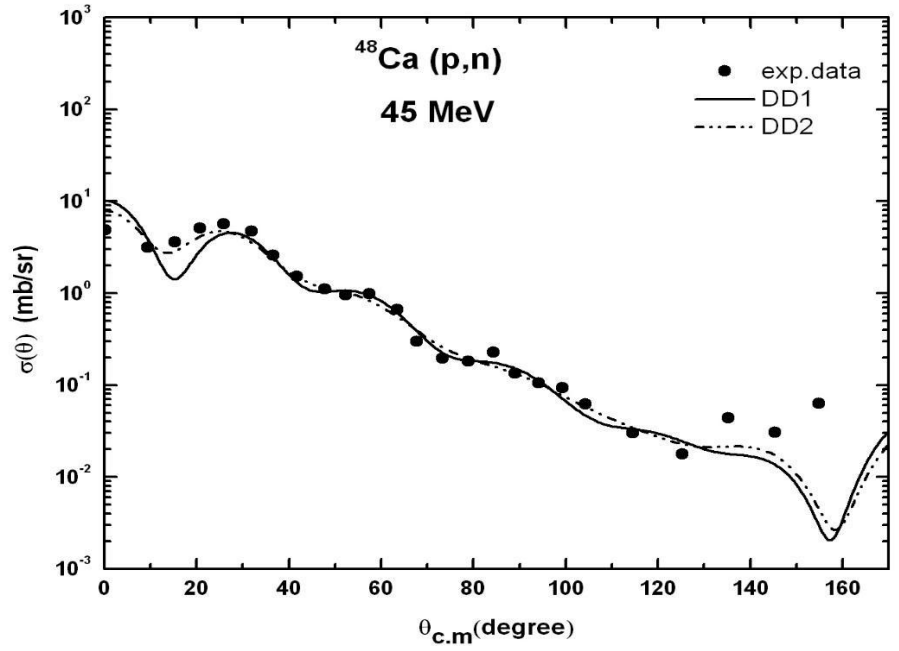

Fig. (9): Quasi-elastic scattering for ^{48}Ca (p,n) at 45 MeV.

The data are taken from Ref.[10].

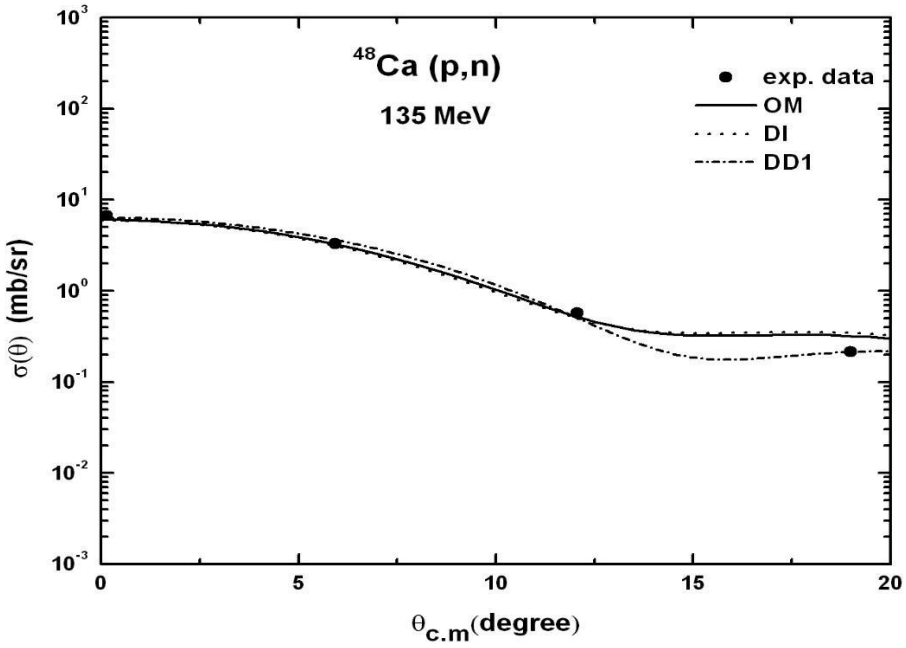

Fig. (10): Quasi-elastic scattering for ^{48}Ca (p,n) at 135 MeV.

The data are taken from Ref.[16].

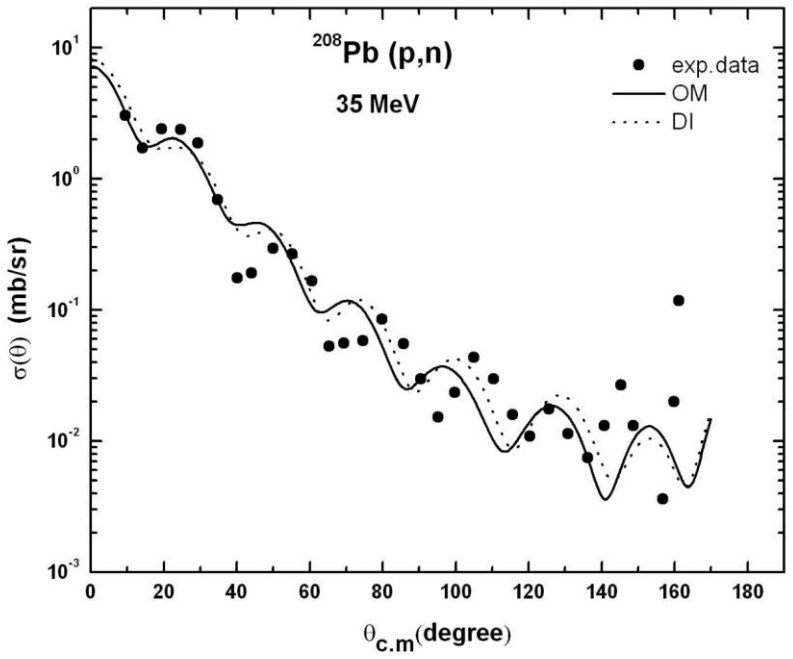

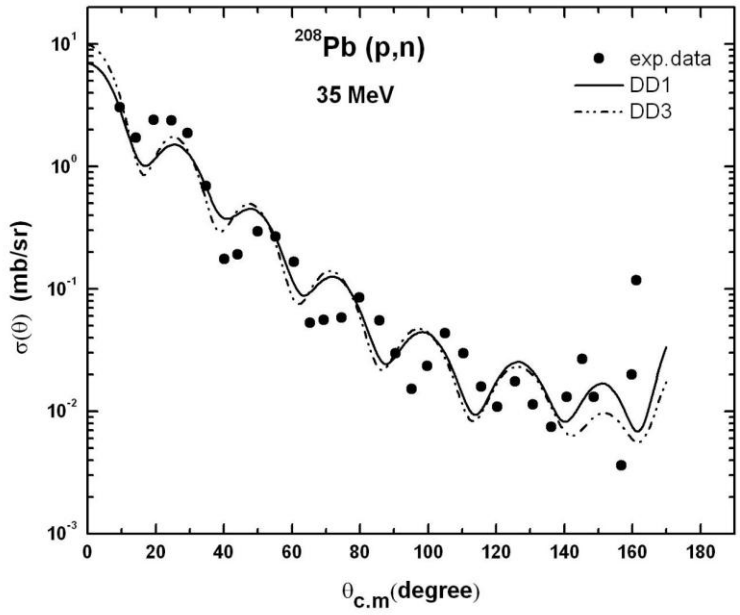

Fig (11): Quasi-elastic scattering for ^{208}Pb (p,n) at 35 MeV.

The data are taken from Ref.[10].

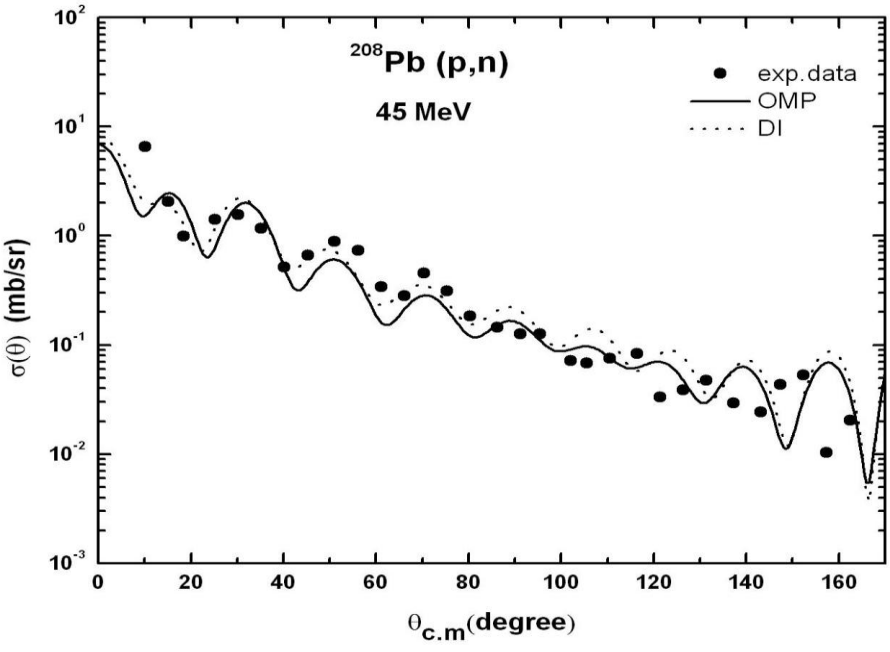

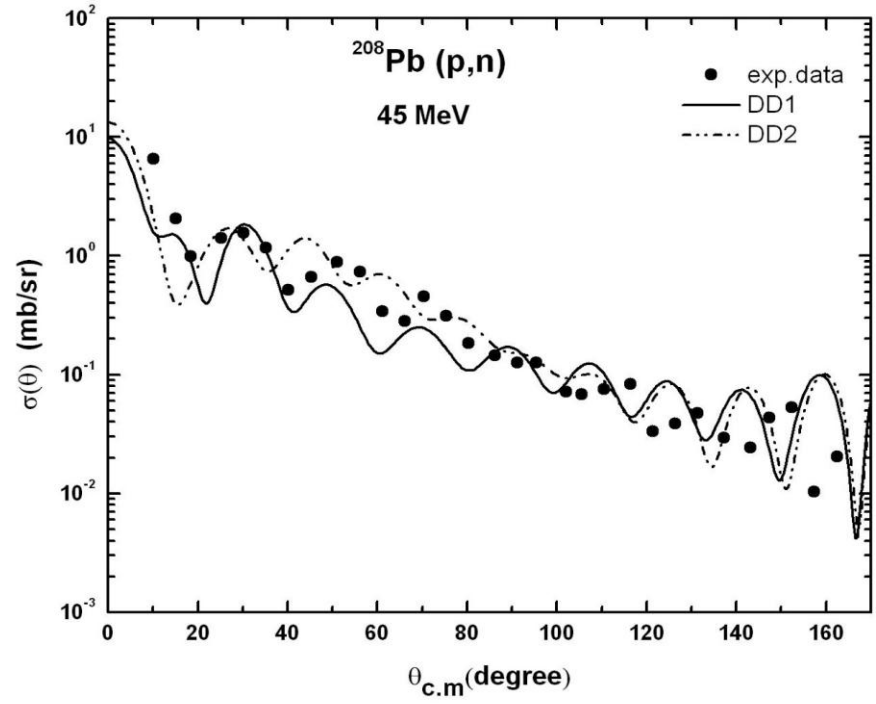

463 Fig (12): Quasi-elastic scattering for ^{208}Pb (p,n) at 45 MeV.

The data are taken from Ref.[10].